JACS
JOURNAL OF THE AMERICAN CHEMICAL SOCIETY

Communication

pubs.acs.org/JACS

Charge Transfer Dynamics between Photoexcited CdS Nanorods and Mononuclear Ru Water-Oxidation Catalysts

Huan-Wei Tseng,‡ Molly B. Wilker,‡ Niels H. Damrauer,* and Gordana Dukovic*

Department of Chemistry and Biochemistry, University of Colorado Boulder, Boulder, Colorado 80309, United States

Supporting Information

ABSTRACT: We describe the charge transfer interactions between photoexcited CdS nanorods and mononuclear water oxidation catalysts derived from the $[Ru(bpy)(tpy)Cl]^+$ parent structure. Upon excitation, hole transfer from CdS oxidizes the catalyst ($Ru^{2+} \rightarrow Ru^{3+}$) on a 100 ps to 1 ns timescale. This is followed by 10−100 ns electron transfer (ET) that reduces the Ru^{3+} center. The relatively slow ET dynamics may provide opportunities for the accumulation of multiple holes at the catalyst, which is necessary for water oxidation.

Using solar photons to drive fuel-generating reactions, such as splitting water into H_2 and O_2, will allow for storage of solar energy necessary for on-demand availability.[1] Inspired by natural photosynthesis, our interest is in exploring artificial systems that feature light absorbers directly coupled with redox catalysts.[2] Colloidal semiconductor nanocrystals are attractive light harvesters because they have tunable absorption spectra and high molar absorptivities (10^5−10^7 $M^{-1}cm^{-1}$). Their coupling with H^+ reduction catalysts has been recently reviewed[2,3] and new studies continue to be reported.[4,5] The resulting hybrid structures are capable of light-driven H_2 generation with the use of sacrificial electron donors. Water oxidation, the other half reaction of water splitting, is a mechanistically complicated process involving the transfer of multiple electrons and protons and the formation of an O−O bond.[6] Over the last three decades, there has been significant progress in the discovery of ruthenium complexes that catalyze water oxidation.[7−13] Consistent with the complexity of this reaction, the molecular catalysts operate at turnover frequencies (TOFs) that are considerably lower than TOFs for H^+ reduction.[2,7] For this reason, successful delivery of photoexcited holes to the catalyst is particularly critical. Understanding the competition between charge transfer and photophysical carrier deactivation pathways, such as electron−hole recombination, is of paramount importance for the design of nanocrystal-based water-splitting systems.

Herein, we describe the charge transfer dynamics between photoexcited CdS nanorods (NRs) and the mononuclear water-oxidation catalyst $[Ru(deeb)(tpy)Cl](PF_6)$ (deeb = diethyl 2,2′-bipyridine-4,4′-dicarboxylate, tpy = 2,2′:6′,2″-terpyridine) in methanol. We refer to the catalyst as complex **1** (Figure 1b). The interaction between the two species results in concentration-dependent quenching of CdS NR photoluminescence (PL) and has a marked impact on CdS excited state dynamics, as measured by transient absorption (TA) spectroscopy. We find that there are two distinct charge transfer steps in the hybrid nanocrystal−catalyst system: hole transfer (HT) followed by electron transfer (ET), both from the photoexcited CdS NR to complex **1**, with the overall result being electron−hole recombination at the metal center. The HT occurs on the timescale of 100 ps to 1 ns, while the subsequent ET occurs in 10−100 ns. The relatively slow rate of recombination exposes opportunities for diverting the photoexcited CdS electrons via auxiliary electron transfer processes.

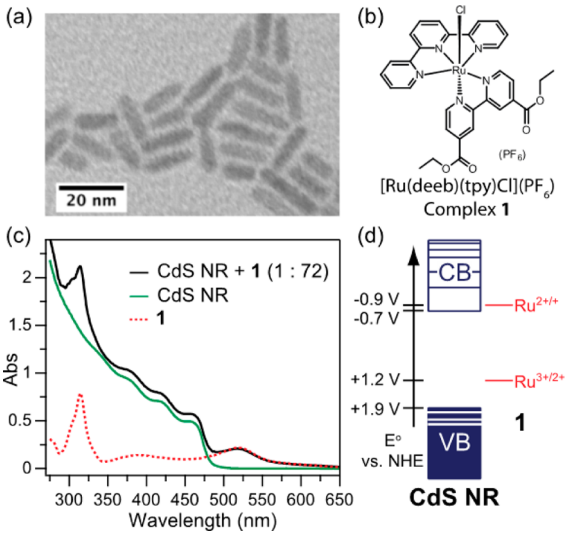

Figure 1. (a) TEM image of CdS NRs with 4.0 ± 0.4 nm widths and 13.7 ± 2.3 nm lengths. (b) Chemical structure of complex **1**. (c) UV−vis absorption spectra of the CdS NRs (1.8×10^{-7} M), complex **1** (1.3×10^{-5} M), and their mixture with a 1:72 NR:**1** molar ratio, all in methanol. (d) Energy level diagram depicting the band edges of CdS NRs and the redox potentials of **1**.

The main design criteria for our model nanocrystal−catalyst system involved: (i) use of materials with relatively well understood optical and catalytic properties, (ii) the possibility of forming electronically coupled heterostructures, and (iii) relative energy alignments that would permit hole transfer from the photoexcited nanocrystal to the catalyst. CdS, a direct-gap semiconductor with a band gap of 2.4 eV, has valence and conduction band positions thermodynamically suitable for both water oxidation and reduction.[14] CdS-based nanostructures have been commonly employed in nanocrystal−catalyst hybrids for H^+ reduction.[2,3] In the selection of a water-oxidation

Received: January 7, 2013

   dx.doi.org/10.1021/ja400178g | J. Am. Chem. Soc. XXXX, XXX, XXX−XXX

catalyst, we took advantage of recent findings demonstrating that the multiple redox steps required for water oxidation can be negotiated by mononuclear ruthenium complexes.[7,10−13] Species based on the $[Ru(bpy)(tpy)Cl]^+$ (bpy = 2,2′-bipyridine) parent structure have the advantages of relatively straightforward synthesis and redox potential tunability via ligand functionalization.[11] The detailed procedures for the experiments discussed here are described in Supporting Information (SI).

The nanocrystals and catalysts were tailored to enable an interaction with sufficient physical proximity for charge transfer in a polar medium. The CdS NRs (Figure 1a) were surface-functionalized with 3-mercaptopropionate (3-MPA)[15] which binds to CdS via the thiolate group while the negatively charged carboxylate prevents flocculation in polar solvents.[16] We modified the $[Ru(bpy)(tpy)Cl]^+$ parent compound with two potential anchoring groups on the bpy: carboxylic acid moieties, based on an approach for attachment of Ru(II) tris-bipyridyl complexes to the surfaces of CdSe quantum dots in organic solvents,[17,18] and ester functionalities (to yield complex **1**), which have been reported to bind to TiO_2.[19] When the Ru complexes were mixed with CdS NRs, the ester functionalities allowed for considerably stronger quenching of CdS PL than the acid groups. This suggests a repulsive interaction between deprotonated carboxylic acid groups on 4,4′-dicarboxy-2,2′-bipyridine and the anionic NR surface capped with 3-MPA. In contrast, complex **1**, with an overall positive charge, may be electrostatically attracted to the NR surface. We note that complex **1** is an active water-oxidation catalyst with relatively high turnover numbers initiated by the sacrificial oxidant Ce^{4+} whose redox potential (1.7 V vs NHE) is less positive than the valence band edge of CdS.[11]

Figure 1c shows the UV−vis absorption spectra of the CdS NRs, complex **1**, and their mixture, all in MeOH. The CdS NR spectrum has four distinct absorption bands, the lowest of which corresponds to the band gap transition at 470 nm (2.64 eV). Complex **1** exhibits a prominent feature that is conveniently located further to the red: a broad absorption band centered at 520 nm attributed to metal-to-ligand charge-transfer.[20] The absorption spectrum of a mixture containing CdS NRs and **1** is a superposition of the spectra of the constituents, indicating that upon mixing, **1** was not chemically modified and CdS NRs were not etched. The mixture was stable to precipitation for at least 24 h. The excitation wavelengths we use for photophysical characterization (360 and 400 nm) primarily excite CdS, with only 4% of absorbed photons exciting **1**. Figure 1d contains an energy level diagram for the CdS-**1** system. Its construction is described in the SI. The $Ru^{3+/2+}$ potential is associated with oxidation at the Ru metal center, while the $Ru^{2+/+}$ is associated with ligand reduction.[21] On the basis of the energy level alignment, we expect hole transfer from photoexcited CdS NRs to the Ru center to be thermodynamically favorable.

The effect of interaction between CdS NRs and **1** on CdS PL is shown in Figure 2. CdS NRs exhibit two distinct PL features: band gap emission (λ_{max} = 475 nm) and trap emission, seen as a broad red-shifted feature.[22,23] The combination of a low quantum yield of exciton emission (<1%) and very long excited electron lifetimes (>100 ns, described below) is an indication of efficient hole trapping.[22,23] Thus, we assign the low-energy trap emission primarily to recombination of a surface-trapped hole with an electron in the lowest CB level. Immediately upon mixing with **1**, both the band gap and trap emission signals

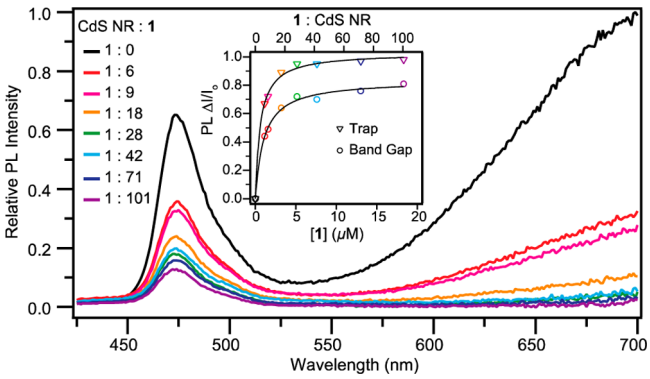

Figure 2. PL spectra of CdS NRs with increasing amounts of **1** and constant [NR] (λ_{ex} = 360 nm). (Inset) Fraction of PL quenched for band gap (475 nm) and trap (700 nm) emission as a function of [**1**] (bottom axis) and the **1**:CdS ratio (top axis). The lines represent fits to a Langmuir adsorption isotherm, suggesting binding between CdS NRs and **1**.

were quenched, with the degree of quenching dependent on the CdS NR:**1** ratio (Figure 2). PL spectra of the mixture remained unchanged for at least 24 h. Complex **1** is nonemissive and remains silent in the PL spectra. In control experiments, PL quenching did not occur upon addition of free tpy or deeb ligands to CdS NRs (Figure S1), thus suggesting the importance of the Ru center in the quenching process.

The inset in Figure 2 illustrates the degree of CdS PL quenching for both the band gap and trap emission signals as a function of **1**:CdS NR ratio. We considered two models for the interaction of CdS NRs and **1**: collisional dynamic quenching, which can be described with a Stern−Volmer expression, and static quenching due to adsorbed molecules, for which a Langmuir adsorption isotherm is suitable (see SI).[18,24] The fit to the Langmuir model is superior (Figure S2), indicating that the quenching behavior is driven at least partially by adsorption. Trap states have considerably longer lifetimes than band gap states,[25] so we expect their emission to be quenched more efficiently. Consequently, the maximum fractional quenching is 1.0 for the former and 0.83 for the latter (Figure 2 inset).

One explanation for the quenching of CdS PL in the presence of **1** is charge transfer. However, since PL intensity depends on the product of electron and hole populations, quenching does not indicate which of the carriers is involved.[17,26] To ascertain the nature of the charge transfer interaction and elucidate the dynamics of this process, we turned to TA spectroscopy over a 100 fs to 1 μs timescale range. TA spectra of CdS NRs (Figure S3a) acquired after 400 nm excitation exhibit a prominent bleach feature (~470 nm) that corresponds to state-filling of the band gap transition. Because the molar absorptivity of **1** is two orders of magnitude smaller than that of CdS NRs, it does not contribute a detectable signal to the TA spectra (Figure S3b,c). We used low pump pulse energies to avoid excitation of multiple electron−hole pairs per NR. The intensity of the 470 nm bleach feature is proportional to the population of excited electrons in the lowest-lying CB level of CdS NRs.[26] This feature is insensitive to the hole population because of the higher density of energy levels near the VB edge.[26] Thus, single-wavelength kinetics at 470 nm can be used as a signature for electron dynamics.

The kinetics of the CdS NR band gap bleach in the presence and absence of **1** are shown in Figure 3a. To facilitate visualization of the dynamics over 7 orders of magnitude in

dx.doi.org/10.1021/ja400178g | J. Am. Chem. Soc. XXXX, XXX, XXX−XXX

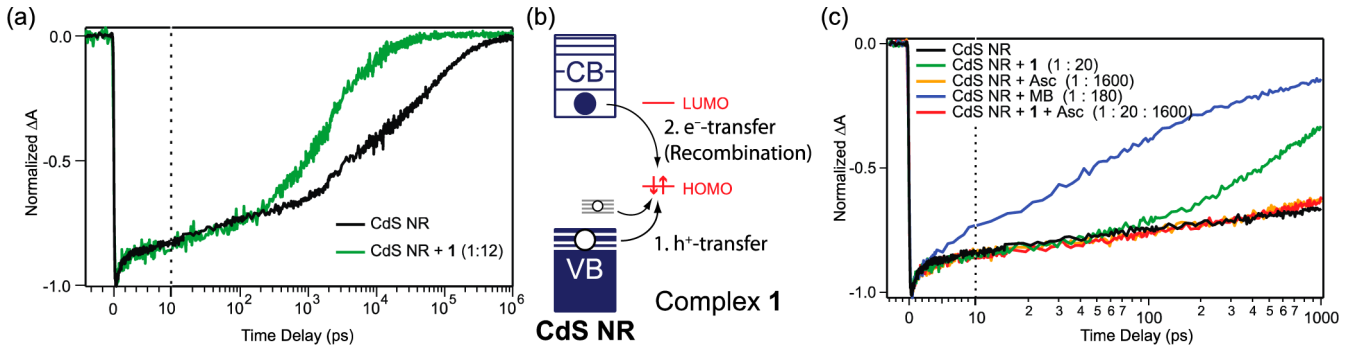

Figure 3. (a) TA decay kinetics at 470 nm for CdS NRs in the presence and absence of **1** (λ_{pump} = 400 nm). The results point to electron transfer that has an onset delayed by 250 ps. (b) Proposed charge transfer steps between photoexcited CdS and **1**. (c) TA decay kinetics at 470 nm for CdS NRs alone, and in the presence of the following: complex **1**, the hole scavenger ascorbate (Asc), the electron acceptor methylene blue (MB), and both **1** and Asc. As described in the text, these kinetic traces are consistent with the charge transfer steps shown in (b).

time, we use a linear time axis up to 10 ps, and a logarithmic scale thereafter. Plots using a linear time axis are shown in Figure S4. Following 400 nm excitation, rapid (~1 ps) electron cooling to the CB edge is observed as a rise of the bleach signal. The subsequent band gap bleach decay of CdS NRs displays multiexponential decay kinetics, consistent with previous reports.[23,27] The bleach kinetics decay to baseline in ~1 μs and exhibit an average lifetime of 160 ns, calculated from a five-exponential fit (see SI). The relatively slow overall electron decay dynamics of CdS NRs have been attributed to a contribution from the slow recombination of the delocalized CB electron with the localized, surface-trapped holes.[23] Addition of **1** in the CdS:**1** ratio of 1:12 has an unusual impact on the electron decay kinetics (Figure 3a). For the first 250 ps, the kinetics of CdS alone and in the presence of **1** are essentially superimposable. Following this, the traces diverge and the electron lifetime is shortened from 160 to 11 ns. This suggests that after a 250 ps delay, additional kinetic pathways become available, enabling ET from CdS to take place.

The 250 ps delay prior to electron lifetime shortening suggests that an electron acceptor state must first be created before ET can take place. On the basis of the energy level diagram in Figure 1d, we hypothesize two sequential charge transfer steps between photoexcited CdS NRs and **1** (Figure 3b): HT from CdS to **1** either directly to or terminating with the metal-centered HOMO (oxidizing Ru^{2+} to Ru^{3+}), followed by ET out of the CdS CB into the newly created available site in the same orbital (reducing Ru^{3+} back to Ru^{2+}). Holes can transfer to **1** from both the VB and trap states, as evidenced by quenching of emission signals associated with both (Figure 2). ET from photoexcited **1** to the CB of CdS would manifest as an additional rise in the bleach signal, and is not observed. We note that a similar lack of change in the early TA dynamics during HT was reported for the case of CdSe nanocrystals coupled to Ru(II) tris-bipyridyl complexes.[17]

To support our hypothesis and the assignment of processes revealed by the TA data, we performed a series of TA experiments using molecular hole and electron acceptors mixed with CdS NRs (Figure 3c). When ascorbate (Asc), a hole scavenger, is added to CdS NRs, no change in the early kinetics of the band gap bleach is observed (Figure 3c, orange trace). This is consistent with the assignment of the bleach to electrons in the CB, and with the lack of HT signature in the TA signal.[17,28] In contrast, when methylene blue (MB), an electron acceptor, is added to CdS NRs, the divergence from the CdS-only trace is observed after 3 ps (Figure 3c, blue trace). This is consistent with a previous report of ET from nanocrystals to MB.[29] These data indicate that the delayed onset of ET in the CdS-**1** system is significantly different from a "pure" ET case, and points to another photoexcited process that precedes ET. Finally, we consider that within our model, the presence of the hole scavenger Asc in the CdS-**1** solution would provide a competing destination for the holes, decrease the population of Ru^{3+}, and circumvent the subsequent ET process. Evidence for this is seen in Figure 3c (red trace) as the lack of the ET signature for CdS + **1** + Asc (i.e., the trace is similar to CdS alone and CdS with Asc). The oxidized form of Asc has an absorption peak at 380 nm,[30] and its accumulation was observed following this TA experiment (Figure S5), indicating that hole transfer to Asc has taken place. We note that the stepwise charge transfer behavior, along with the lack of overlap between CdS emission and **1** absorption, allows us to rule out energy transfer as the mechanism of the PL quenching seen in Figure 2.

The dependence of CdS band gap bleach decay kinetics on the CdS:**1** ratio, with CdS NR concentration held constant, is shown in Figure S6. Over the ratio range of 1:8 to 1:94, the onset time for ET decreases from 370 to 90 ps (Table S1). At the same time, the average electron lifetime decreases from 44 to 1 ns, and the quantum efficiency of ET increases from 72% to 99% (Table S1). As shown in Figure S7, the dependence of these values on the concentration of **1** exhibits saturation behavior similar to that shown in Figure 2 for PL quenching. We do not have enough information to determine the coverage of CdS NRs with **1** under varying mixing ratios. We can, however, estimate that under low-coverage conditions (on the order 1−10 adsorbed molecules per NR), HT occurs on a 100 ps to 1 ns timescale and subsequent ET occurs with at least a 10−100 ns lifetime (see SI). The HT timescale falls within the range of observed values for HT from Cd-chalcogenide nanocrystals to molecular hole acceptors (5 ps to 50 ns) with a variety of coupling conditions and relative energy level alignments.[2] The ET, on the other hand, is significantly slower than values previously reported for common electron acceptors such as viologens, MB, and polyaromatic quinones, which are typically <100 ps.[2] The relatively slow ET may be due to a combination of low wave function overlap between the hole localized on Ru^{3+} and the electron delocalized in a CdS NR, significantly different electronic couplings for the HT and the ET pathways, and the very large driving force for ET (~1.9 eV) placing the process in the Marcus inverted regime. Further

dx.doi.org/10.1021/ja400178g | J. Am. Chem. Soc. XXXX, XXX, XXX−XXX

work is needed to elucidate the factors that determine the HT and ET rates in this system.

These results have significant implications for photochemical water splitting. Under the conditions of our current experiment, the metal center acts as a recombination site where each HT event that oxidizes Ru^{2+} is followed by an ET event that reduces the site. However, the ET timescale is relatively slow. We propose that additional pathways can be designed to funnel away photoexcited electrons and allow for the accumulation of multiple holes on the catalyst, thereby facilitating O−O bond formation. Examples of potential electron destinations include molecular acceptors and catalysts for H^+ reduction.[2] Furthermore, built-in charge separation in the so-called type-II nanoheterostructures could assist in electron removal from the nanocrystal.[2] The nanocrystal/water-oxidation catalyst hybrid could serve as a unit in a more complex photochemical water-splitting architecture. Additionally, we expect that improved understanding of the binding equilibria between CdS NRs and catalysts will allow us to negotiate the competition for holes among multiple catalysts on each NR. Finally, we note that efficient delivery of photoexcited holes to the water-oxidation catalysts may have the added benefit of preventing nanocrystal photo-oxidation.

In summary, we have described the charge transfer interactions between photoexcited CdS NRs and the water-oxidation catalyst [Ru(deeb)(tpy)Cl](PF$_6$). We have found evidence for a stepwise charge transfer mechanism that involves hole transfer from photoexcited CdS to the HOMO of [Ru(deeb)(tpy)Cl](PF$_6$), occurring on a 100 ps to 1 ns timescale, followed by electron transfer from the conduction band of CdS to the same orbital on [Ru(deeb)(tpy)Cl](PF$_6$), which is considerably slower at 10−100 ns. The second step could be averted through introduction of additional electron harvesting pathways.

■ ASSOCIATED CONTENT

Supporting Information

Experimental; construction of Figure 1d energy level diagram; PL of CdS NRs with free ligands of **1**; discussion of concentration-dependent PL quenching; TA spectra of CdS with and without **1**; data in Figure 3a on a linear time axis; absorption spectra showing Asc oxidation; concentration-dependent TA kinetics. This material is available free of charge via the Internet at http://pubs.acs.org.

■ AUTHOR INFORMATION

Corresponding Author

Gordana.Dukovic@colorado.edu; Niels.Damrauer@colorado.edu

Author Contributions

‡These authors contributed equally.

Notes

The authors declare no competing financial interest.

■ ACKNOWLEDGMENTS

We gratefully acknowledge funding support from the Renewable and Sustainable Energy Institute (RASEI), NSF CAREER grant no. CHE-1151151 (M.B.W. and G.D.), and the King Family Fellowship at CU and the A.P. Sloan Foundation (N.H.D. and H.-W.T.).

■ REFERENCES

(1) Lewis, N. S.; Nocera, D. G. *Proc. Natl. Acad. Sci. U.S.A.* **2006**, *103*, 15729.
(2) Wilker, M. B.; Schnitzenbaumer, K. J.; Dukovic, G. *Isr. J. Chem.* **2012**, *52*, 1002.
(3) Chen, X. B.; Shen, S. H.; Guo, L. J.; Mao, S. S. *Chem. Rev.* **2010**, *110*, 6503.
(4) Han, Z.; Qiu, F.; Eisenberg, R.; Holland, P. L.; Krauss, T. D. *Science* **2012**, *338*, 1321.
(5) Huang, J.; Mulfort, K. L.; Du, P.; Chen, L. X. *J. Am. Chem. Soc.* **2012**, *134*, 16472.
(6) Weinberg, D. R.; Gagliardi, C. J.; Hull, J. F.; Murphy, C. F.; Kent, C. A.; Westlake, B. C.; Paul, A.; Ess, D. H.; McCafferty, D. G.; Meyer, T. J. *Chem. Rev.* **2012**, *112*, 4016.
(7) Concepcion, J. J.; Jurss, J. W.; Brennaman, M. K.; Hoertz, P. G.; Patrocinio, A. O. T.; Iha, N. Y. M.; Templeton, J. L.; Meyer, T. J. *Acc. Chem. Res.* **2009**, *42*, 1954.
(8) Wada, T.; Tsuge, K.; Tanaka, K. *Angew. Chem., Int. Ed.* **2000**, *39*, 1479.
(9) Sens, C.; Romero, I.; Rodriguez, M.; Llobet, A.; Parella, T.; Benet-Buchholz, J. *J. Am. Chem. Soc.* **2004**, *126*, 7798.
(10) Zong, R.; Thummel, R. P. *J. Am. Chem. Soc.* **2005**, *127*, 12802.
(11) Tseng, H. W.; Zong, R.; Muckerman, J. T.; Thummel, R. *Inorg. Chem.* **2008**, *47*, 11763.
(12) Duan, L. L.; Fischer, A.; Xu, Y. H.; Sun, L. C. *J. Am. Chem. Soc.* **2009**, *131*, 10397.
(13) Wasylenko, D. J.; Ganesamoorthy, C.; Koivisto, B. D.; Henderson, M. A.; Berlinguette, C. P. *Inorg. Chem.* **2010**, *49*, 2202.
(14) Nozik, A. J. *Annu. Rev. Phys. Chem.* **1978**, *29*, 189.
(15) Brown, K. A.; Wilker, M. B.; Boehm, M.; Dukovic, G.; King, P. W. *J. Am. Chem. Soc.* **2012**, *134*, 5627.
(16) Aldana, J.; Lavelle, N.; Wang, Y.; Peng, X. *J. Am. Chem. Soc.* **2005**, *127*, 2496.
(17) Sykora, M.; Petruska, M. A.; Alstrum-Acevedo, J.; Bezel, I.; Meyer, T. J.; Klimov, V. I. *J. Am. Chem. Soc.* **2006**, *128*, 9984.
(18) Koposov, A. Y.; Szymanski, P.; Cardolaccia, T.; Meyer, T. J.; Klimov, V. I.; Sykora, M. *Adv. Funct. Mater.* **2011**, *21*, 3159.
(19) Kelly, C. A.; Farzad, F.; Thompson, D. W.; Meyer, G. J. *Langmuir* **1999**, *15*, 731.
(20) Christopoulos, K.; Karidi, K.; Tsipis, A.; Garoufis, A. *Inorg. Chem. Commun.* **2008**, *11*, 1341.
(21) Jakubikova, E.; Chen, W. Z.; Dattelbaum, D. M.; Rein, F. N.; Rocha, R. C.; Martin, R. L.; Batista, E. R. *Inorg. Chem.* **2009**, *48*, 10720.
(22) Peng, P.; Sadtler, B.; Alivisatos, A. P.; Saykally, R. J. *J. Phys. Chem. C* **2010**, *114*, 5879.
(23) Wu, K. F.; Zhu, H. M.; Liu, Z.; Rodriguez-Cordoba, W.; Lian, T. Q. *J. Am. Chem. Soc.* **2012**, *134*, 10337.
(24) Munro, A. M.; Jen-La Plante, I.; Ng, M. S.; Ginger, D. S. *J. Phys. Chem. C* **2007**, *111*, 6220.
(25) Klimov, V. I.; Schwarz, C. J.; McBranch, D. W.; Leatherdale, C. A.; Bawendi, M. G. *Phys. Rev. B* **1999**, *60*, R2177.
(26) Klimov, V. I. *Annu. Rev. Phys. Chem.* **2007**, *58*, 635.
(27) Knowles, K. E.; McArthur, E. A.; Weiss, E. A. *ACS Nano* **2011**, *5*, 2026.
(28) Huang, J. E.; Huang, Z. Q.; Jin, S. Y.; Lian, T. Q. *J. Phys. Chem. C* **2008**, *112*, 19734.
(29) Huang, J.; Huang, Z. Q.; Yang, Y.; Zhu, H. M.; Lian, T. Q. *J. Am. Chem. Soc.* **2010**, *132*, 4858.
(30) Warren, J. J.; Mayer, J. M. *J. Am. Chem. Soc.* **2010**, *132*, 7784.